Higgs boson production via gluon fusion at hadron colliders

Stefano Catani

INFN, Sezione di Firenze and Dipartimento di Fisica, Università di Firenze, I-50019 Sesto Fiorentino, Florence, Italy

Abstract. We consider Higgs boson production, through gluon fusion, in hadron collisions at the Tevatron and the LHC. We present a brief summary of the calculations of QCD radiative corrections to this process. We show available theoretical predictions for the total cross section and the transverse-momentum distribution of the Standard Model Higgs boson. The perturbative QCD uncertainty on these predictions is discussed.

1. INTRODUCTION

Within the Standard Model (SM) of electroweak interactions, the Higgs boson is responsible for the mechanism of the electroweak symmetry breaking. This particle has so far eluded experimental discovery. The next search for Higgs boson(s) will be carried out at hadron colliders, namely, the Fermilab Tevatron [1, 2] and the CERN LHC [3, 4].

The main production mechanism of the SM Higgs boson H at hadron colliders is the gluon fusion process $gg \to H$, through a heavy-quark (mainly, top-quark) loop. When combined with the decay channels $H \to \gamma\gamma$, $H \to WW$ and $H \to ZZ$, this production mechanism is one of the most important for Higgs boson searches and studies over the entire mass range, 100 GeV $\lesssim M_H \lesssim$ 1 TeV, to be investigated at the LHC [3]. The gluon fusion mechanism is also important for Higgs boson searches at the Tevatron: in the mass range 140 GeV $\lesssim M_H \lesssim$ 180 GeV, the process $gg \to H \to WW \to \ell^+\ell^-\nu\bar{\nu}$ can be exploited as main discovery channel [1], provided the background from $t\bar{t}$ production is suppressed by applying a veto cut on the transverse momenta of the jets accompanying the final-state leptons.

To fully exploit the physics potential of the gluon fusion process, it is relevant to provide reliable theoretical predictions for the corresponding total cross section and for the associated distributions, such as, for instance, the Higgs transverse-momentum (q_T) distribution. The dominant source of theoretical uncertainties on these quantities is the effect of QCD radiative corrections, which, therefore, have to be carefully investigated.

2. TOTAL CROSS SECTION

In QCD perturbation theory, the leading order (LO) contribution to the total cross section for Higgs boson production by gluon fusion is proportional to α_S^2, α_S being the QCD coupling. The next-to-leading order (NLO) QCD corrections to this process were found to be large [5, 6]: their effect increases the LO cross section by about 80–100$\%$, thus leading to very uncertain predictions. Approximate evaluations [7] of higher-order terms suggested that they could still be sizeable.

Recent years have witnessed much theoretical progress [8]–[17] on the computation of QCD radiative corrections beyond the NLO. The total cross section has been computed at the next-to-next-to-leading order (NNLO) [12]. The Higgs boson rapidity distribution has been computed at the NLO [14] and at the NNLO [15, 16]. The effects of a jet veto on the NLO and NNLO cross sections have been studied [11, 13, 15]. Note that all these results [8]–[17] use the large-M_t approximation, M_t being the mass of the top quark (the validity of this approximation is discussed below).

A key point of this theoretical activity is that the QCD dynamics of the gluon fusion mechanism has been understood. The origin of the dominant perturbative contributions to the total cross section has been identified: the bulk of the radiative corrections is due to virtual and soft-gluon terms [7, 9, 10, 11]. On the contrary, as shown and discussed in Sects. 4.1 and 5.1 of Ref. [17] (see, in particular, Figs. 1 and 2 in [17]), the contribution from hard-gluon radiation to the total cross section is marginal: it is of $\mathcal{O}(10\%)$ and of $\mathcal{O}(1\%)$ at NLO and NNLO, respectively.

The dominance of virtual and soft-gluon terms has a twofold relevance. On one side, it explains the observation [7] of the validity of the large-M_t approximation (M_t is certainly much larger than the energy scale of the soft gluons that mainly contribute to the QCD radiative corrections) in the calculation at the NLO, and, therefore, it justifies the use of the same approximation at and beyond the NNLO. On the other side, it allows to estimate higher-order QCD contributions by supplementing the NNLO calculation with an all-order resummation of the logarithmically-enhanced terms due to multiple soft-gluon emission. Having these terms under control allows us to reliably predict the value of the cross section and, more importantly, to reduce the associated perturbative uncertainty.

The general method to systematically resum classes of logarithmically-enhanced soft-gluon contributions to hadroproduction cross sections is known [18, 19].

In Ref. [17], the total cross section at NNLO is supplemented with the resummation of the soft-gluon contributions up to next-to-next-to-leading logarithmic (NNLL) accuracy. The NNLO and NNLL cross sections at the LHC are reported in Fig. 1. The central curves are obtained by fixing the factorization (μ_F) and renormalization (μ_R) scales at the default value $\mu_F = \mu_R = M_H$. The bands are obtained by varying μ_F and μ_R simultaneously and independently in the range $0.5M_H \leq \mu_F, \mu_R \leq 2M_H$ with the constraint $0.5 \leq \mu_F/\mu_R \leq 2$. Tables with detailed numerical values of Higgs boson cross sections (using also different sets of NNLO parton densities) at the LHC and at the Tevatron can be found in Ref. [17]. The NNLL cross sections are larger than the NNLO ones; the increase is of about 6% at the LHC and varies from about 12% (when $M_H = 100$ GeV) to about 15% (when $M_H = 200$ GeV) at the Tevatron. For comparison, we recall that the NNLO results increase the NLO results by about 20% at the LHC and about 40% at the Tevatron. At the LHC, the NNLO scale dependence ranges from about $\pm 10\%$ when $M_H = 120$ GeV, to about $\pm 9\%$ when $M_H = 200$ GeV. At NNLL order, it is about $\pm 8\%$ when $M_H \lesssim 200$ GeV. At the Tevatron, when $M_H \lesssim 200$ GeV, the NNLO scale dependence is about $\pm 13\%$, whereas the NNLL scale dependence is about $\pm 8\%$. It is important to observe that the NNLO and NNLL bands overlap. Furthermore, the central value of the NNLL bands lies inside the corresponding NNLO bands. This gives us con-

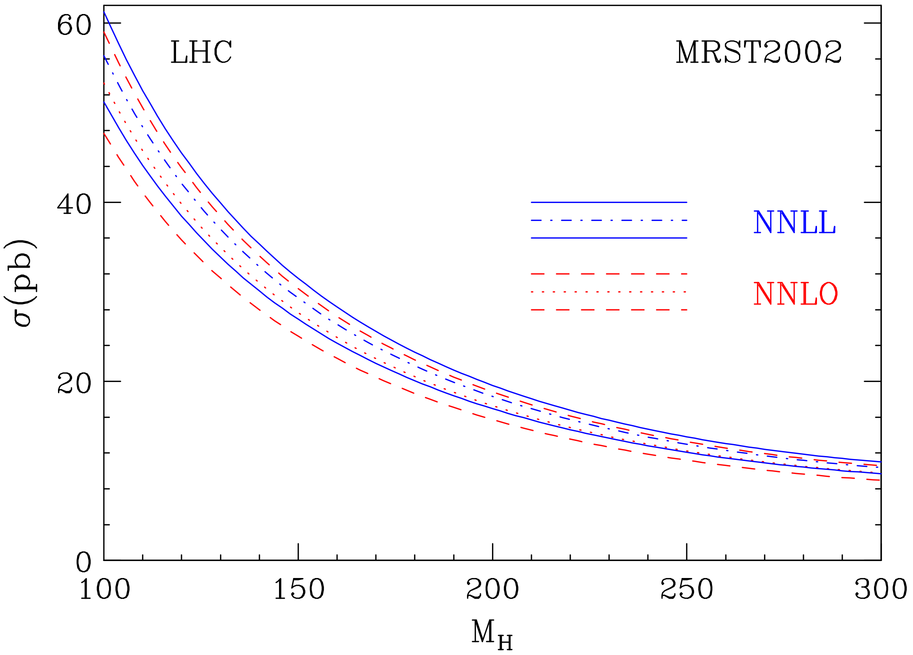

FIGURE 1. NNLL and NNLO cross sections at the LHC, using MRST2002 [20] parton densities.

fidence in using scale variations at NNLO and at NNLL order to estimate the theoretical uncertainty due to uncalculated perturbative terms at still higher orders. Another method to estimate the size of higher-order corrections is to compare the results at the highest order that is available with those at the previous order. Considering the differences between the NNLO and NNLL cross sections, we obtain results that are consistent with the uncertainty estimated from scale variations.

In summary, after inclusion of both NNLO corrections and soft-gluon resummation at the NNLL level, we can reliably predict the Higgs boson production cross section. In the low-mass range ($M_H \lesssim 200$ GeV), the estimated theoretical uncertainties of perturbative QCD origin are below 10% [17].

The NNLL+NNLO results are nicely confirmed by the recent computation [21] of part of the N^{3}LO and N^{3}LL perturbative contributions (see also Ref. [22, 23]).

3. TRANSVERSE-MOMENTUM DISTRIBUTION

When studying the q_T distribution of the Higgs boson in QCD perturbation theory, it is convenient to start by considering separately the large-q_T and small-q_T regions.

The large-q_T region is identified by the condition $q_T \sim M_H$. In this region, the perturbative series is controlled by a small expansion parameter, $\alpha_S(M_H^2)$, and calculations based on the truncation of the series at a fixed order in α_S are theoretically justified. SM Higgs boson production at large q_T via gluon fusion has to be accompanied by the radiation of at least one recoiling parton, so the LO term for this observable is proportional to α_S^3. The LO calculation was reported in Ref. [24]; it shows that the large-M_t approximation works well as long as $M_H \lesssim 2M_t$ and $q_T \lesssim M_t$. Similar results on the validity of the large-M_t approximation were obtained in the case of the associated production of a Higgs boson plus 2 jets (2 recoiling partons at large transverse momenta) [25]. In the framework of the large-M_t approximation, the NLO QCD corrections to the transverse-momentum distribution of the SM Higgs boson were computed in Refs. [26]–[29]. Corrections to the large-M_t approximation are considered in Ref. [30]. The numerical programs of Refs. [26, 29] can also be used to evaluate arbitrary infrared- and collinear-safe observables up to NLO in the large-q_T region and, in the case of Ref. [29], up to NNLO when $q_T = 0$.

At large values of q_T, the NLO calculation increases the LO result by about 60%. This implies that further higher-order terms (e.g. the NNLO term) in QCD perturbation theory have to be evaluated to improve the accuracy of the predictions in the large-q_T region.

In the small-q_T region ($q_T \ll M_H$), where the bulk of events is produced, the convergence of the fixed-order expansion is definitely spoiled, since the coefficients of the perturbative series in $\alpha_S(M_H^2)$ are enhanced by powers of large logarithmic terms, $\ln^m(M_H^2/q_T^2)$. These logarithmic terms are due to multiple emission of soft and collinear gluons (i.e. gluons with low transverse momentum). To obtain reliable perturbative predictions, these terms have to be resummed to all orders in α_S. The method to systematically perform all-order resummation of classes of logarithmically-enhanced terms at small q_T is known [31]–[37]. In the case of the SM Higgs boson, resummation has been explicitly worked out at leading logarithmic (LL), next-to-leading logarithmic (NLL) [38, 39] and next-to-next-to-leading logarithmic (NNLL) [40] level.

The fixed-order and resummed approaches at small and large values of q_T can then be matched at intermediate values of q_T, to obtain QCD predictions for the entire range of transverse momenta. Phenomenological studies of the SM Higgs boson q_T distribution have been performed in Refs. [39, 41]–[49], by combining resummed and fixed-order perturbation theory at different levels of theoretical accuracy. A comparison of theoretical calculations and of results from parton shower Monte Carlo generators is presented in Ref. [50].

In Refs. [46, 49], the Higgs boson q_T distribution at the LHC is computed by combining the most advanced perturbative information that is available at present: NNLL resummation at small q_T and NLO perturbation theory at large q_T. The formalism used in the calculation is illustrated in detail in Ref. [49]. The resummed and fixed-order contributions are matched by avoiding double-counting of perturbative terms. A constraint of perturbative unitarity is imposed on the resummed terms, so that the total cross section at the nominal NNLO (or NLO) accuracy is recovered upon integration over q_T of the transverse-momentum spectrum at NNLL+NLO (or NLL+LO) accuracy. This unitarity constraint has the purpose of reducing the effect of unjustified higher-order contributions (those introduced by the resummed terms) at large values of q_T and, especially, at intermediate values of q_T.

An example of the quantitative studies[1] presented in Ref. [49] is reported in Fig. 2.

---

[1] The calculation of Ref. [49] is implemented in the numerical code `HqT`, which can be downloaded from the url `http://arturo.fi.infn.it/grazzini/codes.html`

Considering Higgs boson ($M_H = 125$ GeV) production at the LHC, the q_T spectrum at NNLL+NLO accuracy is compared to that at the previous order, namely NLL+LO accuracy, in the resummed perturbative expansion. The computed q_T spectra have a physical behaviour when $q_T \to 0$ and a kinematical peak at $q_T \sim 12$ GeV. The NNLL+NLO and NLL+LO bands are obtained by performing variations of the factorization and renormalization scales as in Fig. 1 (see also Sect. 2). At NLL+LO accuracy, the scale dependence increases from about $\pm 15\%$ at the peak to about $\pm 20\%$ at $q_T = 100$ GeV. At NNLL+NLO accuracy, the scale dependence is about $\pm 8\%$ at the peak and increases to about $\pm 20\%$ at $q_T = 100$ GeV. The inset plot shows the NNLL+NLO band normalized to the NLL+LO result at central value of the scales. From the inset plot, we see that the q_T spectrum at NNLL+NLO accuracy is slightly harder than at NLL+LO accuracy; the ratio between the NNLL+NLO and NLL+LO cross section is stable, around the values 1.1–1.2, in the region 5 GeV$\lesssim q_T \lesssim 50$ GeV. Note that the NNLL+NLO band is smaller than the NLL+LO one, and the former is included in (overlaps with) the latter at $q_T \lesssim 50$ GeV ($q_T \lesssim 100$ GeV): this suggests a good convergence of the resummed perturbative expansion. The results in Fig. 2 are obtained in a purely perturbative framework. Non-perturbative effects on the q_T spectrum are estimated in Refs. [49, 52]: they are definitely below 10% when $q_T \gtrsim 10$ GeV and decrease very rapidly as q_T increases.

In summary, the comparison of the NLL+LO and NNLL+NLO results from small (around the peak region) to intermediate (say, roughly, $q_T \lesssim M_H/3$) values of transverse momenta shows a nice convergence of the resummed QCD predictions for the q_T spectrum of the Higgs boson at the LHC. From this comparison and from the effects of scale variations, we conclude [49] that the perturbative QCD uncertainty of the NNLL+NLO results is *uniformly* of about 10% *over* this range of transverse momenta.

4. CONCLUDING REMARKS

In recent years much theoretical progress has been made on the calculation of QCD radiative corrections to the gluon fusion mechanism for Higgs boson production at hadron colliders. Reliable and accurate theoretical predictions are presently available for the total cross section and the transverse-momentum distribution of the SM Higgs boson.

After inclusion of both NNLO corrections and soft-gluon resummation at the NNLL level, the theoretical uncertainties of perturbative origin in the calculation of the total cross section at the Tevatron and at the LHC are below 10% in the low-mass range ($M_H \lesssim 200$ GeV). The differences (and the uncertainties) obtained by using various sets of available parton densities can, however, reach values that, at present, are larger than 10% (see Ref. [17]).

The transverse-momentum distribution of the Higgs boson can be computed [49] by including the resummation (at the NNLL level) of the logarithmically-enhanced terms at small q_T and the fixed-order expansion (at the NLO level) of the perturbative terms at large q_T. The integral over q_T of the transverse-momentum distribution at NNLL+NLO level reproduces the total cross section at NNLO. At the LHC, the perturbative QCD uncertainty on the q_T spectrum at NNLL+NLO accuracy is uniformly of about 10% from small (around the peak region) to intermediate (say, roughly, $q_T \lesssim M_H/3$) values of

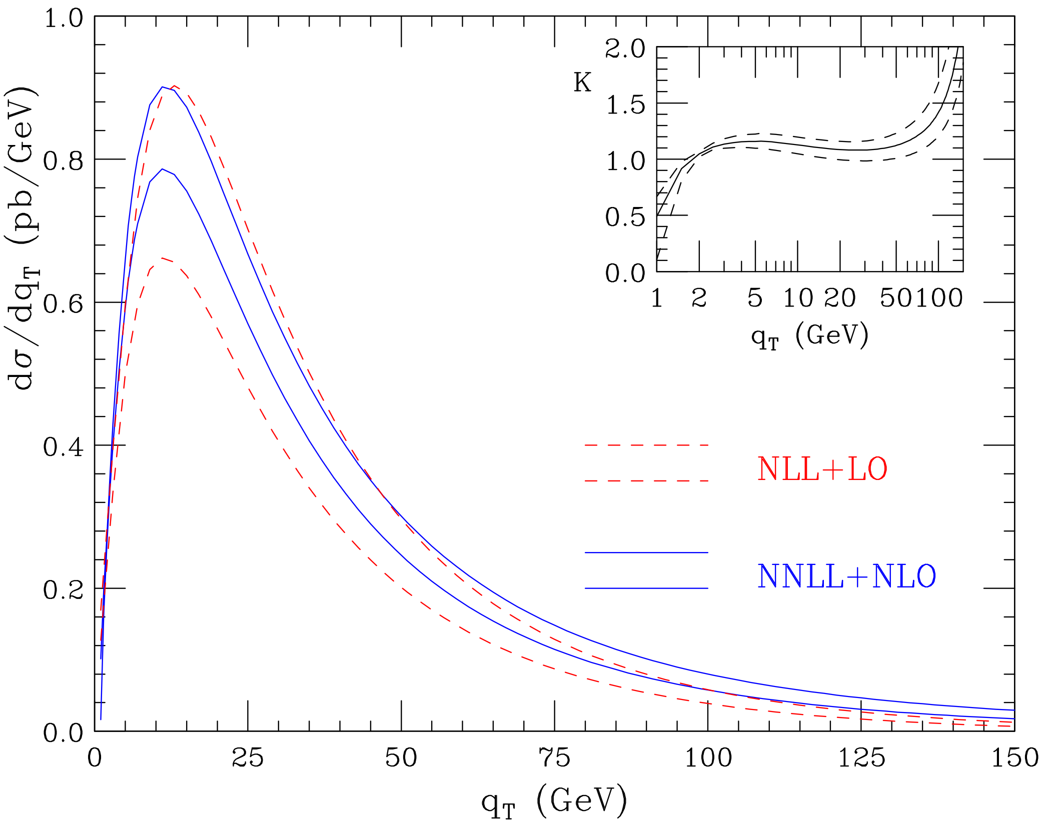

FIGURE 2. The q_T spectrum of the Higgs boson ($M_H = 125$ GeV) at the LHC. Comparison of the NNLL+NLO and NLL+LO results, using MRST2004 [51] parton densities. The inset plot shows the NNLL+NLO band normalized to the central value of the NLL+LO result.

q_T. The uncertainty due to perturbative and non-perturbative effects increases at smaller values of q_T; the perturbative uncertainty increases also at larger values of q_T.

ACKNOWLEDGMENTS

I am very pleased to thank Pietro Colangelo, Fulvia De Fazio, Eugenio Nappi and Beppe Nardulli for their great organization of this nice Workshop. I wish to thank Daniel, Giuseppe, Massimiliano and Paolo for the scientific collaboration on the topics discussed in this talk.

REFERENCES

1. M. Carena *et al.*, *Report of the Tevatron Higgs working group*, hep-ph/0010338; CDF and D0 Collaborations, *Results of the Tevatron Higgs Sensitivity Study*, report FERMILAB–PUB–03/320-E.
2. W. M. Yao [CDF and D0 Collaborations], report FERMILAB–CONF–04/307-E [hep-ex/0411053].
3. CMS Coll., *Technical Proposal*, report CERN/LHCC/94-38 (1994); ATLAS Coll., *ATLAS Detector and Physics Performance: Technical Design Report*, Vol. 2, report CERN/LHCC/99-15 (1999).

4. S. Abdullin *et al.*, report CMS-NOTE-2003-033; S. Asai *et al.*, Eur. Phys. J. C **32S2** (2004) 19.
5. S. Dawson, Nucl. Phys. B **359** (1991) 283; A. Djouadi, M. Spira and P. M. Zerwas, Phys. Lett. B **264** (1991) 440.
6. M. Spira, A. Djouadi, D. Graudenz and P. M. Zerwas, Nucl. Phys. B **453** (1995) 17.
7. M. Kramer, E. Laenen and M. Spira, Nucl. Phys. B **511** (1998) 523.
8. R. V. Harlander, Phys. Lett. B **492** (2000) 74; V. Ravindran, J. Smith and W. L. van Neerven, Nucl. Phys. B **704** (2005) 332.
9. S. Catani, D. de Florian and M. Grazzini, JHEP **0105** (2001) 025.
10. R. V. Harlander and W. B. Kilgore, Phys. Rev. D **64** (2001) 013015.
11. S. Catani, D. de Florian and M. Grazzini, JHEP **0201** (2002) 015.
12. R. V. Harlander and W. B. Kilgore, Phys. Rev. Lett. **88** (2002) 201801; C. Anastasiou and K. Melnikov, Nucl. Phys. B **646** (2002) 220; V. Ravindran, J. Smith and W. L. van Neerven, Nucl. Phys. B **665** (2003) 325.
13. S. Catani, D. de Florian and M. Grazzini, hep-ph/0206052, in *2002 QCD and hadronic interactions*, Proceedings of the 37th Rencontres de Moriond: QCD and Hadronic Interactions, 37th, Les Arcs, France, March 2002.
14. C. Anastasiou, L. J. Dixon and K. Melnikov, Nucl. Phys. Proc. Suppl. **116** (2003) 193.
15. C. Anastasiou, K. Melnikov and F. Petriello, Phys. Rev. Lett. **93** (2004) 262002.
16. C. Anastasiou, these Proceedings.
17. S. Catani, D. de Florian, M. Grazzini and P. Nason, JHEP **0307** (2003) 028.
18. G. Sterman, Nucl. Phys. B **281** (1987) 310; S. Catani and L. Trentadue, Nucl. Phys. B **327** (1989) 323, Nucl. Phys. B **353** (1991) 183.
19. S. Catani, M. L. Mangano, P. Nason and L. Trentadue, Nucl. Phys. B **478** (1996) 273.
20. A. D. Martin, R. G. Roberts, W. J. Stirling and R. S. Thorne, Phys. Lett. B **531** (2002) 216.
21. S. Moch and A. Vogt, report DESY-05-152 [hep-ph/0508265].
22. E. Laenen and L. Magnea, report DFTT-26-2005[hep-ph/0508284].
23. A. Idilbi, X. d. Ji, J. P. Ma and F. Yuan, report RBRC–562 [hep-ph/0509294].
24. R. K. Ellis, I. Hinchliffe, M. Soldate and J. J. van der Bij, Nucl. Phys. B **297** (1988) 221; U. Baur and E. W. Glover, Nucl. Phys. B **339** (1990) 38.
25. V. Del Duca, W. Kilgore, C. Oleari, C. Schmidt and D. Zeppenfeld, Nucl. Phys. B **616** (2001) 367, Phys. Rev. D **67** (2003) 073003.
26. D. de Florian, M. Grazzini and Z. Kunszt, Phys. Rev. Lett. **82** (1999) 5209.
27. V. Ravindran, J. Smith and W. L. Van Neerven, Nucl. Phys. B **634** (2002) 247.
28. C. J. Glosser and C. R. Schmidt, JHEP **0212** (2002) 016.
29. C. Anastasiou, K. Melnikov and F. Petriello, report UH-511-1066-05 [hep-ph/0501130].
30. J. Smith and W. L. van Neerven, Nucl. Phys. B **720** (2005) 182.
31. Y. L. Dokshitzer, D. Diakonov and S. I. Troian, Phys. Rep. **58** (1980) 269.
32. G. Parisi and R. Petronzio, Nucl. Phys. B **154** (1979) 427.
33. G. Curci, M. Greco and Y. Srivastava, Nucl. Phys. B **159** (1979) 451.
34. J. C. Collins and D. E. Soper, Nucl. Phys. B **193** (1981) 381 [Erratum-ibid. B **213** (1983) 545], Nucl. Phys. B **197** (1982) 446; J. C. Collins, D. E. Soper and G. Sterman, Nucl. Phys. B **250** (1985) 199.
35. J. Kodaira and L. Trentadue, Phys. Lett. B **112** (1982) 66, report SLAC-PUB-2934 (1982), Phys. Lett. B **123** (1983) 335.
36. S. Catani, D. de Florian and M. Grazzini, Nucl. Phys. B **596** (2001) 299.
37. E. Laenen, G. Sterman and W. Vogelsang, Phys. Rev. D **63** (2001) 114018.
38. S. Catani, E. D'Emilio and L. Trentadue, Phys. Lett. B **211** (1988) 335.
39. R. P. Kauffman, Phys. Rev. D **45** (1992) 1512.
40. D. de Florian and M. Grazzini, Phys. Rev. Lett. **85** (2000) 4678, Nucl. Phys. B **616** (2001) 247.
41. I. Hinchliffe and S. F. Novaes, Phys. Rev. D **38** (1988) 3475.
42. R. P. Kauffman, Phys. Rev. D **44** (1991) 1415.
43. C. P. Yuan, Phys. Lett. B **283** (1992) 395; C. Balazs and C. P. Yuan, Phys. Lett. B **478** (2000) 192.
44. C. Balazs, J. Huston and I. Puljak, Phys. Rev. D **63** (2001) 014021.
45. E. L. Berger and J. w. Qiu, Phys. Rev. D **67** (2003) 034026, Phys. Rev. Lett. **91** (2003) 222003.
46. G. Bozzi, S. Catani, D. de Florian and M. Grazzini, Phys. Lett. B **564** (2003) 65.
47. A. Kulesza and W. J. Stirling, JHEP **0312** (2003) 056.
48. A. Kulesza, G. Sterman and W. Vogelsang, Phys. Rev. D **69** (2004) 014012.

49. G. Bozzi, S. Catani, D. de Florian and M. Grazzini, report LPSC 05–63 [hep-ph/0508068].
50. C. Balazs, M. Grazzini, J. Huston, A. Kulesza and I. Puljak, hep-ph/0403052, published in M. Dobbs *et al.*, hep-ph/0403100, p. 51, Proceedings of the Les Houches 2003 Workshop on *Physics at TeV Colliders*.
51. A. D. Martin, R. G. Roberts, W. J. Stirling and R. S. Thorne, Phys. Lett. B **604** (2004) 61.
52. G. Bozzi, S. Catani, D. de Florian and M. Grazzini, in K. A. Assamagan *et al.* [Higgs Working Group Collaboration], hep-ph/0406152, p. 14, proceedings of the Les Houches 2003 Workshop on *Physics at TeV Colliders*.